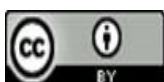


DOI: <http://doi.org/10.52716/jprs.v12i1.600>

Fabrication of a Gas Sensor from Thin Films of Tungsten Oxide Nanoparticles and Their Use in Oil Refineries

Khalid. H. JeburMinistry of Oil - Oil Training Institute - Baghdad – Iraq
Correspondent Author Email: khaled7005b.rrrrrttrrrrr@gmail.com6th Iraq Oil and Gas Conference, 29-30/11/2021This work is licensed under a [Creative Commons Attribution 4.0 International License](https://creativecommons.org/licenses/by/4.0/).

Abstract

In this research, the structural and sensitivity properties of the toxic gases of films tungsten oxide (WO_3) nanoparticles prepared by the pulsed laser deposition method were manufactured and studied using a Nd:YAG laser. To show the effect of different temperatures (400, 600 and 800 °C) on films deposited on quartz substrate for all samples. The results of X-Ray diffraction (XRD) showed that all the thin films have polycrystalline structure and have a peak direction (010) for all samples, and that increasing the temperature led to an increase in the particle size. The decrease in the values of the full width and half maximum (FWHM) of the films (WO_3) for (010) modes from 0.19 to 0.14 with increasing temperature. The nature of the topography of tungsten oxide (WO_3) nanoparticles was studied using atomic force microscopy (AFM), which proved that the films grown in this way have good crystallization and have a homogeneous surface. The root mean square (RMS) values of the tungsten oxide nanoparticles (WO_3) increases with increasing temperature. When measuring the sensitivity of tungsten oxide nanoparticles (WO_3) to (CO , NH_3 and NO_2) gases, it was found that the films have good sensitivity to these gases at room temperature (RT), and it was the best sensitivity of the films is at a temperature of (800 °C) as follows: CO gas (81%), NH_3 gas (84%) and NO_2 gas (100%). All studies have shown that tungsten oxide (WO_3) has the ability to detect toxic gases, such as (CO , NH_3 and NO_2), which have a detrimental effect on workers in oil refineries. The films of tungsten oxide (WO_3) is used in the manufacture of gas sensors that can be used in these refineries, and when the temperature increases, it becomes more sensitive to gases (CO , NH_3 , NO_2).

Keywords: Tungsten oxide (WO_3), pulsed laser, nanoparticles, pulsed laser, (PLD).

تصنيع مستشعر الغاز من الاغشية الرقيقة لجسيمات أكسيد التنجستن النانوية واستخدامها في مصافي النفط

الخلاصة:

في هذا البحث تم تصنيع ودراسة الخصائص التركيبية والحساسية للغازات السامة لأغشية جزيئات أكسيد التنجستن النانوية لإظهار تأثير درجات الحرارة المختلفة (400، 600، 800) درجة مئوية، المحضرة بطريقة الترسيب بالليزر النبضي باستخدام ليزر Nd: YAG على الأفلام المترسبة على ركيزة الكوارتز لجميع العينات. أظهرت نتائج حيود الأشعة السينية (XRD) ان جميع الاغشية الرقيقة لها بنية متعددة البلورات ولها اتجاه ذروة (010) لجميع العينات. وأن زيادة درجة الحرارة أدت إلى زيادة حجم الجسيمات عند (010) من 0.19 الى 0.14 مع زيادة درجة WO_3 لاغشية (FWHM) انخفاض قيم العرض الكامل عند منتصف القمة AFM باستخدام مجهر القوة الذرية WO_3 . تمت دراسة طبيعة تضاريس الجسيمات النانوية من أكسيد التنجستن والتي أثبتت أن الاغشية المزروعة بهذه الطريقة لها تبلور جيد ولها سطح متجانس. تزداد قيم جذر متوسط التربيع (RMS) لجسيمات أكسيد التنجستن النانوية (WO_3) مع زيادة درجة الحرارة. عند قياس حساسية الجسيمات النانوية لأوكسيد التنجستن (WO_3) لغازات (CO، NO_2 ، NH_3)، وجد أن الفلم لديها حساسية جيدة لهذه الغازات عند درجة حرارة الغرفة (RT)، وكانت أفضل حساسية. عند درجة حرارة الفلم (800) درجة مئوية كالتالي: غاز اول أكسيد الكربون (81%)، غاز NH_3 (84%) وغاز NO_2 (100%). أظهرت جميع الدراسات أن أكسيد التنجستن (WO_3) لديها القدرة على اكتشاف الغازات السامة، مثل (NH_3 ، NO_2)، والتي لها تأثير ضار على العاملين في مصافي النفط. تستخدم أغشية أكسيد التنجستن (WO_3) في تصنيع مستشعرات الغاز التي يمكن استخدامها في هذه المصافي، وعندما ترتفع درجة الحرارة، تصبح أكثر حساسية للغازات (NO_2 ، NH_3 ، CO).

1. Introduction

(WO_3) is a semiconductor metallic oxide with a band gap of 2.9 eV, which has been used in different applications, like savvy windows, electronic data shows, electrochromic devices, gas sensors and photo catalyst, photovoltaic devices and photograph electrochemical devices [1–5].

For the preparation of tungsten oxide film, various deposition techniques were used, for example chemical vapor deposition [6,7], pulsed laser deposition [8,9], spray pyrolysis [10,11], electrodeposition [12], spin coating [13], sol–gel methods [14,15], sputtering [16,17], thermal evaporation [18,19] and oxidation of W films [20]. Pulsed laser deposition (PLD) has been used in the preparation of tungsten oxide films over classical deposition methods due to its many advantages, including good adhesion to substrate deposition temperature, reproducibility, controllability of stoichiometry and crystal structure, and thus direct deposition of alloys and compounds of materials with different vapor pressures.

The aim of study focuses on the deposition of WO_3 films on quartz substrates by PLD, and the detailed investigation of the influence of different temperatures on the structural, morphological and sensitivity properties of the deposited WO_3 films and used it as applications in gas sensors. A gas sensor was manufactured to give an audible signal when the amount of gases emitted from the equipment is increased in oil places.

2-Experimental part

In this study, WO_3 powder with a purity of 99.99% was pressed by a hydraulic press for 15 minutes at a pressure of 7 tons, resulting in a disc with a diameter of 1.5 cm and 2 mm thick. Quartz substrates (1.5×1.5 cm) were used to deposit the tungsten oxide film. Distilled water was used to clean them and remove the remaining dust and dirt from their surface. Then the substrates were cleaned with alcohol for 5 min by the ultrasonic system to remove some oxides and grease.

Hot air was used in this process to dry the quartz substrates, and finally, fine paper was used to wipe the slides. An ND:YAG laser was applied to film deposition using pulsed laser deposition (PLD) technique with a wavelength (1064 nm) and energy of 800 mJ and a rate of 1000 pulses by different temperatures at (400, 600 and 800 °C) for all samples as the Figure (1).

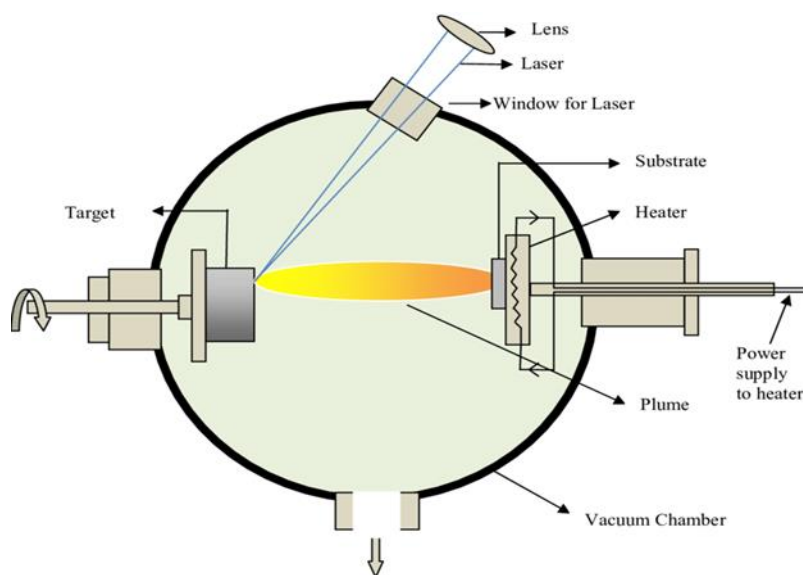


Fig. (1): Pulsed laser deposition system[21]

3. Result and discussion

3.1 X-ray diffraction (XRD)

X-ray diffraction (XRD) spectra of WO_3 nanostructures thin films grown at various temperatures substrate (400, 600 and 800°C). All the diffraction peaks in this pattern Figure (2) can be indexed to the monoclinic polycrystalline structure according to the JCPDS card no 00-5-0386. As well the temperature difference plays a role in the composition of crystalline levels whether mono-crystalline or polycrystalline or random crystalline in addition to the dependence on the type of precipitated base. The reasons for the low rate of crystallization can only be due to the type of nucleus formed between the atoms of the thin film material or because at the specific heat at the solid body or because of different melting points of the components of the material or thermodynamic properties of the mixture which are consistent with the reference.

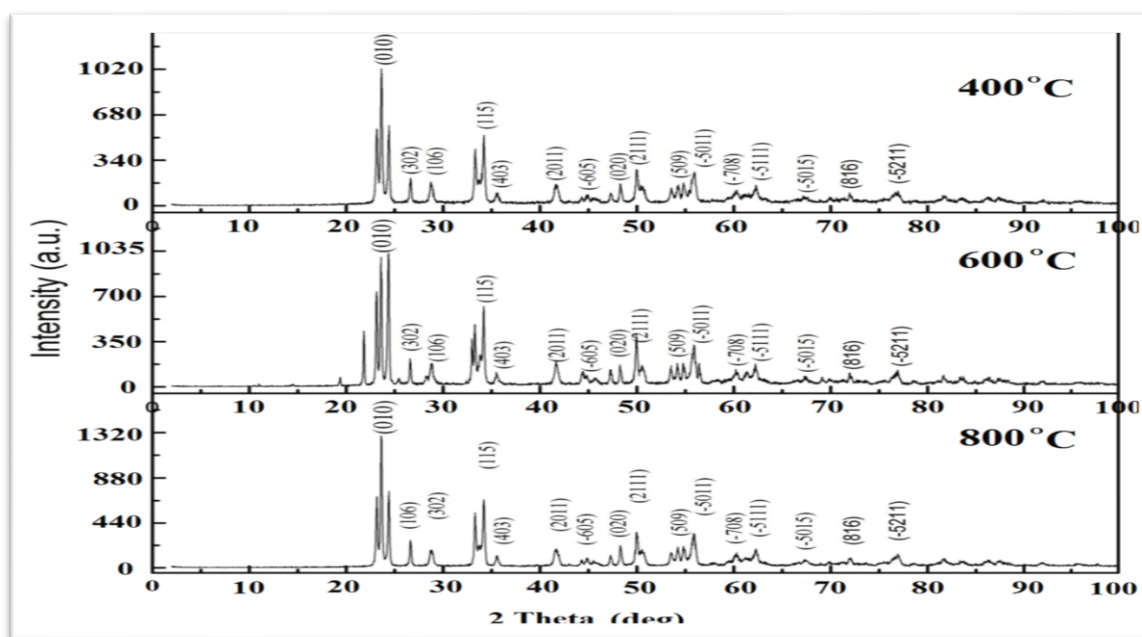


Fig.(2): X-ray diffraction patterns of WO_3 nanoparticles thin films at various temperatures substrate (400, 600 and 800 °C)

The crystallite size can be calculate from the Scherrer equation, which is expressed as:

$$D = 0.94 \lambda / \beta \cos \theta.$$

where (D) is the crystallite size, (θ) is the diffraction angle, (β) is the FWHM of diffraction peak, $\lambda = 1.5406 \text{ \AA}$ is the wavelength of Cu $K\alpha$ radiation and Scherrer's constant is ($K = 0.94$).

Using the above equation, the crystallite size of WO_3 was calculated for different temperatures substrate, as shown in the Table below.

Table(1) Crystallite size at various temperatures substrate of WO_3 nanostructure thin films.

Temperatures Substrate (° C)	Crystallite Size (nm)
400	40.5
600	50.2
800	57.9

3.2 Atomic force microscopy (AFM)

The AFM images give some quantitative data about the surface roughness (R) and the maximum height of the WO_3 nanoparticles thin films were prepared at different temperatures substrate(400, 600 and 800 °C) as shown in Figures (3).

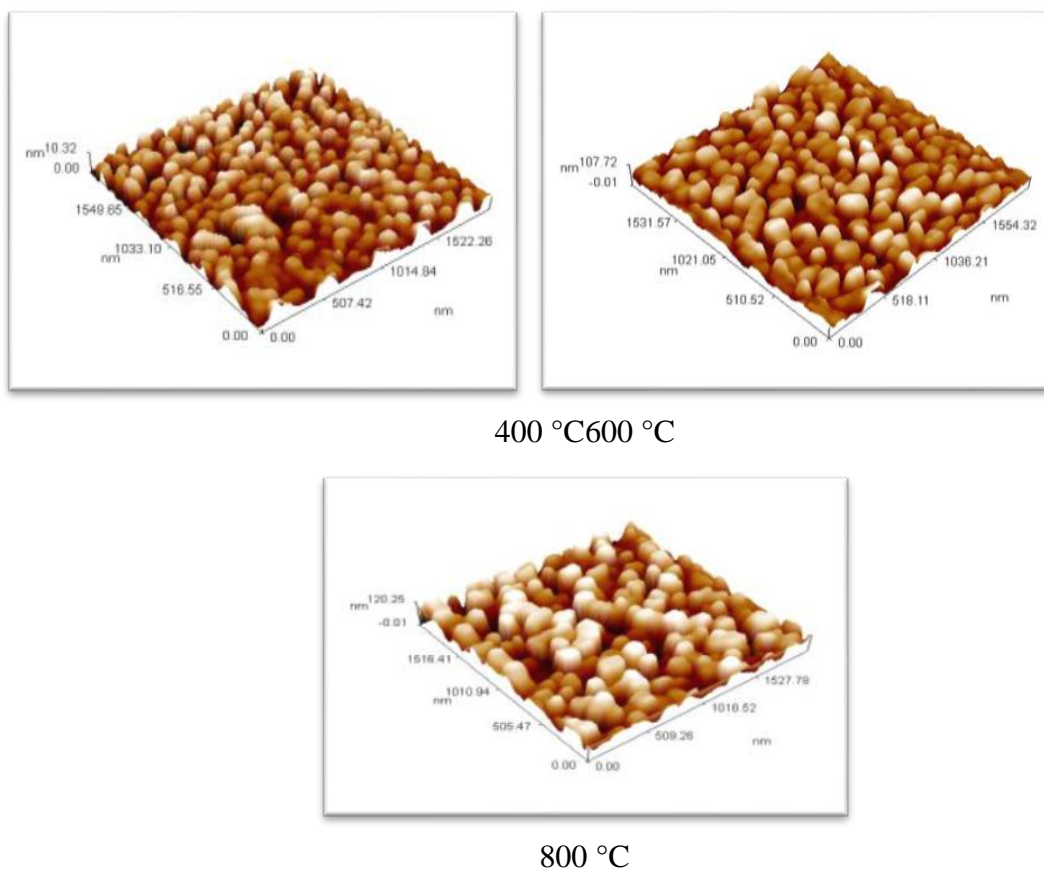


Fig.(3): The AFM images of WO_3 nanoparticles thin films at various temperatures substrate (400, 600 and 800 °C).

The obtained of surface roughness (R) values showed in Table(2).

Table(2) Morphological characteristics from AFM images for WO₃nanoparticles thin films

Temperatures Substrate °C	roughness (R) (nm)	RMS(nm)
400	12	43.1
600	17.3	56.7
800	27	69.2

The minimum value of surface roughness and (RMS) of films at 400 k and increase with increasing temperature as shown in Table (2) indicating that the temperature increases growth and makes the surface of films free of voids and homogeneous distribution for grains.

The surface roughness value and (RMS) will increase and the grain size becomes larger, the reason for this is high temperature facilitates the coalescence of the surface grains and therefore rougher surface and thus an increase in the grain size.

3.3Optical measurements

The transmittance spectra and absorbance as a function of the wavelength in the range between (200-1100) nm were investigated to the WO₃ nanostructure thin films. By increasing the temperature substrate, a decrease in transmittance was observed in most samples, and vice versa with respect to the absorption of these films, as shown in the Figure (4).

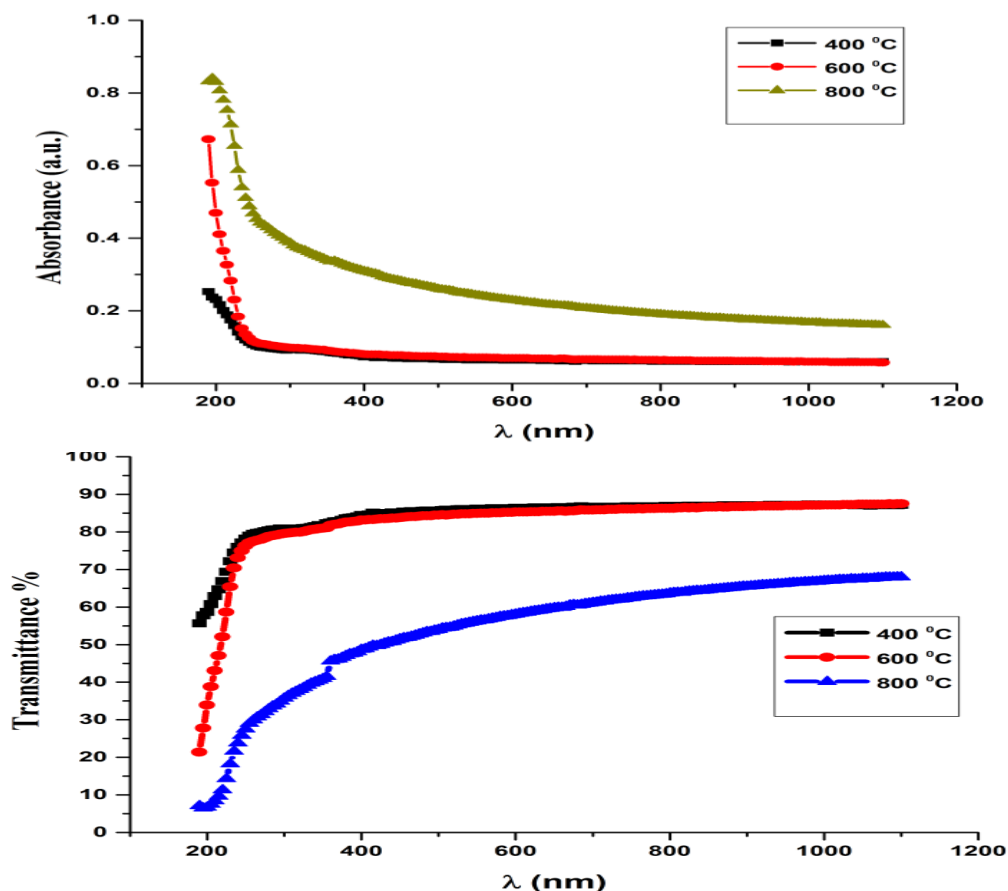


Fig.(4):Transmittance and absorbance spectra of WO₃ nanoparticles thin film at different temperature substrate(400, 600 and 800 °C)

As the shapes of the formed nanostructures change with the increase of the temperature substrate, the transmittance of the prepared samples are found to strongly depend on the aggregate shape. The prepared samples demonstrate more than 80% transmittance at wavelengths longer than 240 nm for the temperature substrate about of (400, 600 and 800 °C) and decreases sharply below 240 nm that is indicated to the light scattering of the films in this region as the temperature substrate increases.

The optical energy gap of WO₃ is calculated from the model of Tauc [22]

$$\alpha h\nu = B (h\nu - E_g)^n$$

where (α) absorption coefficient, (B) the transition constant is equal to one, (n) equal (1/2) for the allowed direct transition. The energy band gap was determined by extrapolating the linear state of the plot of $(\alpha h\nu)^2$ versus $(h\nu)$ on the energy axis, as shown in Figure (5).

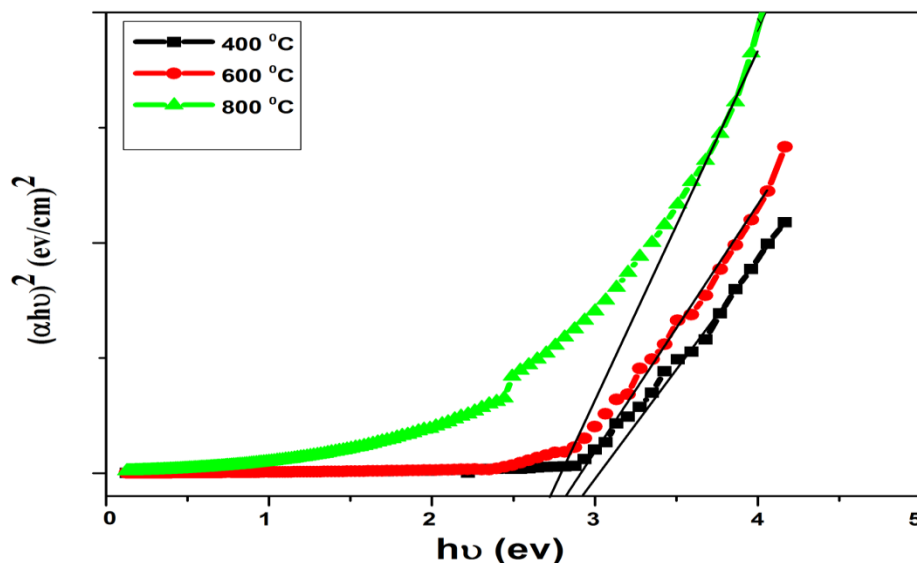


Fig.(5): The optical band gap of WO_3 nanoparticles thin films at different temperature substrate (400, 600 and 800 °C).

For all samples the energy band gap decreases when the temperature substrate increase, as shown in the Table (3).

Table (3): The optical band gap of WO_3 nanoparticles thin films at different temperature substrate (400, 600 and 800 °C).

Temperatures Substrate °C	Band gap (ev)
400	2.9
600	2.8
800	2.7

3.4 sensing measurements

The gas sensing properties were evaluated by measuring the changes of resistance of the sensors, before and after enter the gases. The measurements have been room temperature (RT). Figures (6), (7) and (8) shows dynamic response curves of the sensors based on (50,100 and 150) ppm at varying (CO , NH_3 and NO_2) gases concentrations at room temperature.

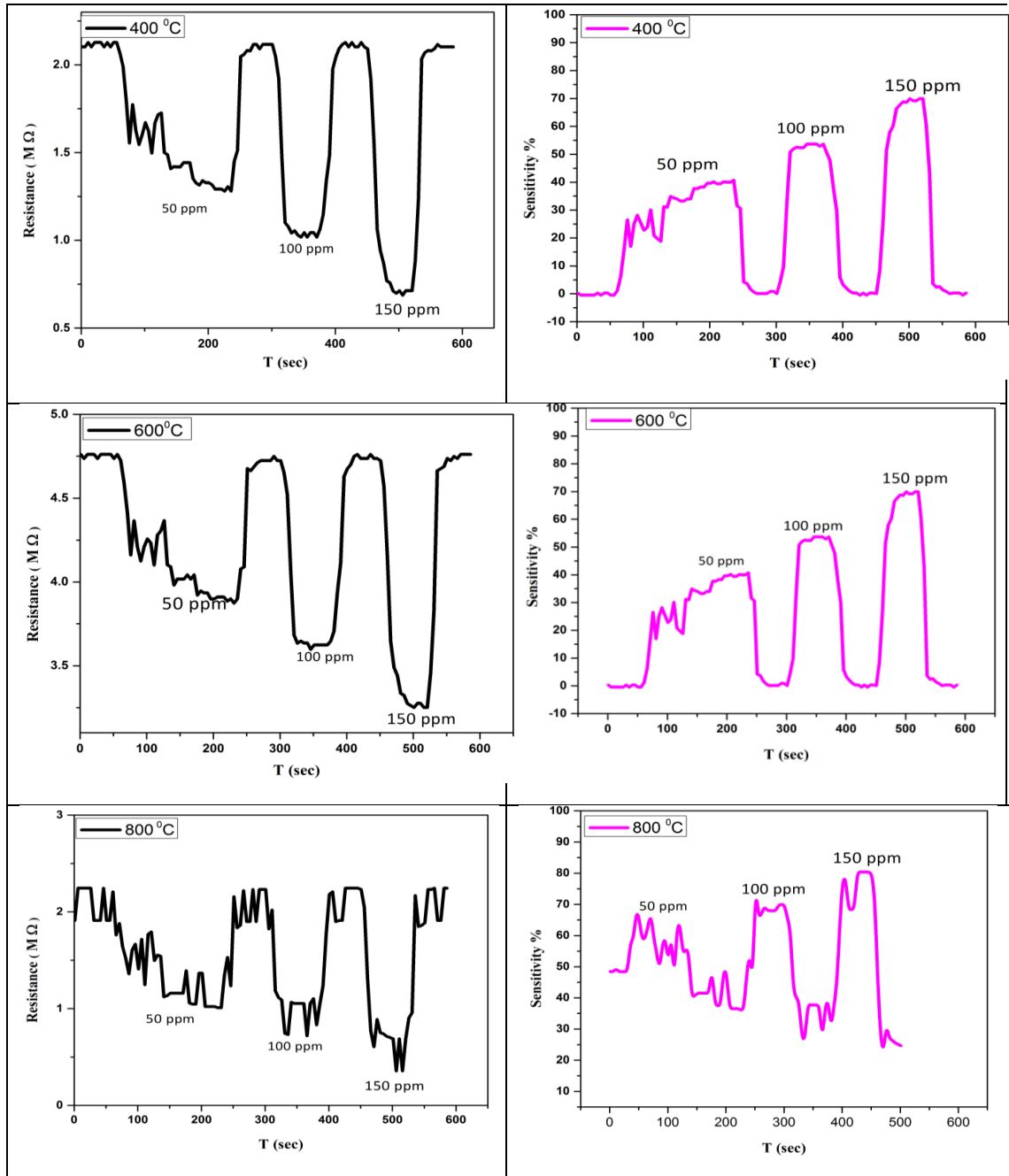


Fig. (6): Resistance and Sensitivity for the COgas for the samples that treated at different temperatures substrate 400 °C, 600 °C and 800 °C,

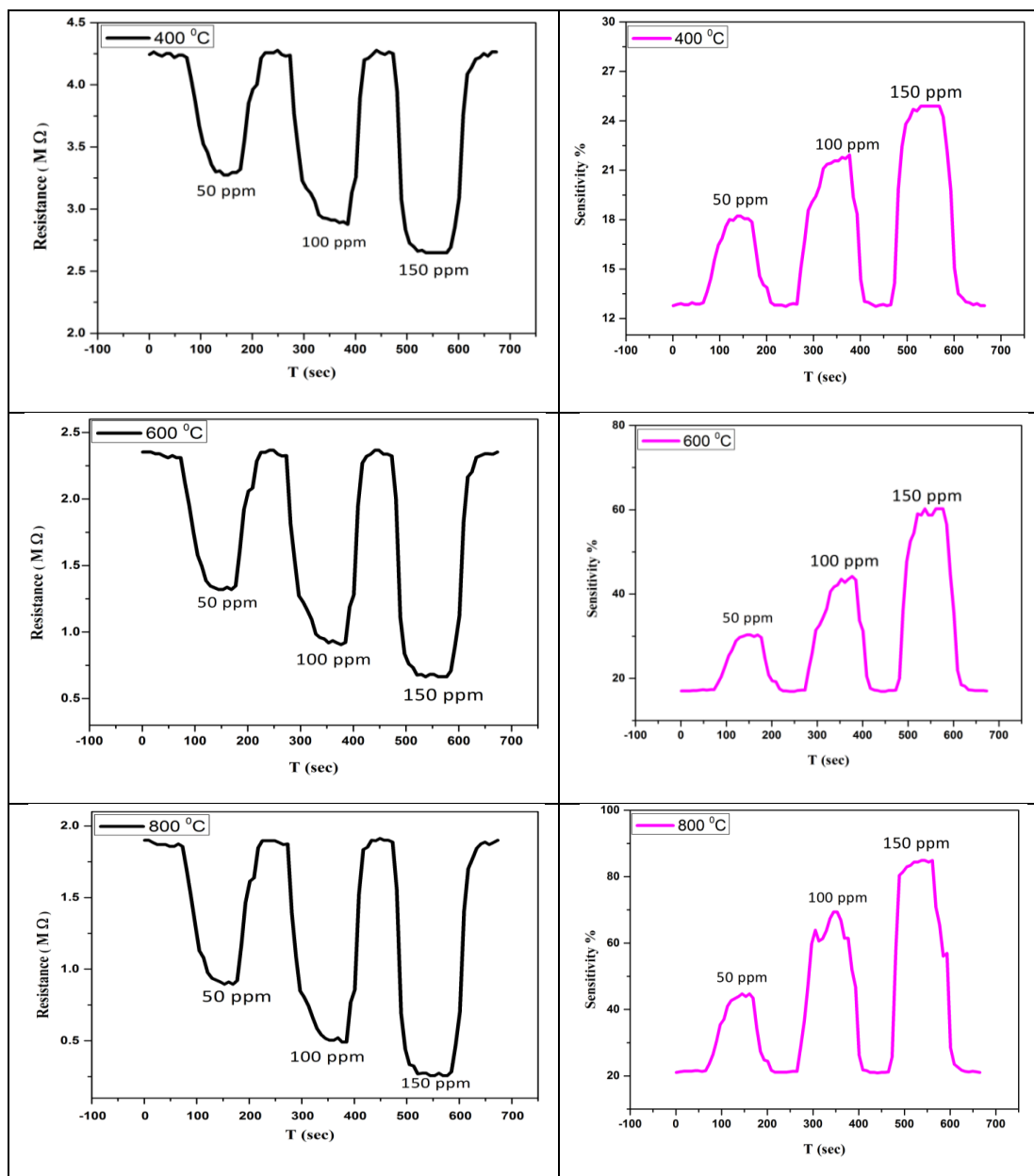


Fig. (7): Resistance and Sensitivity for the NH₃ gas for the samples that treated at different temperatures substrate 400 °C, 600 °C and 800 °C,

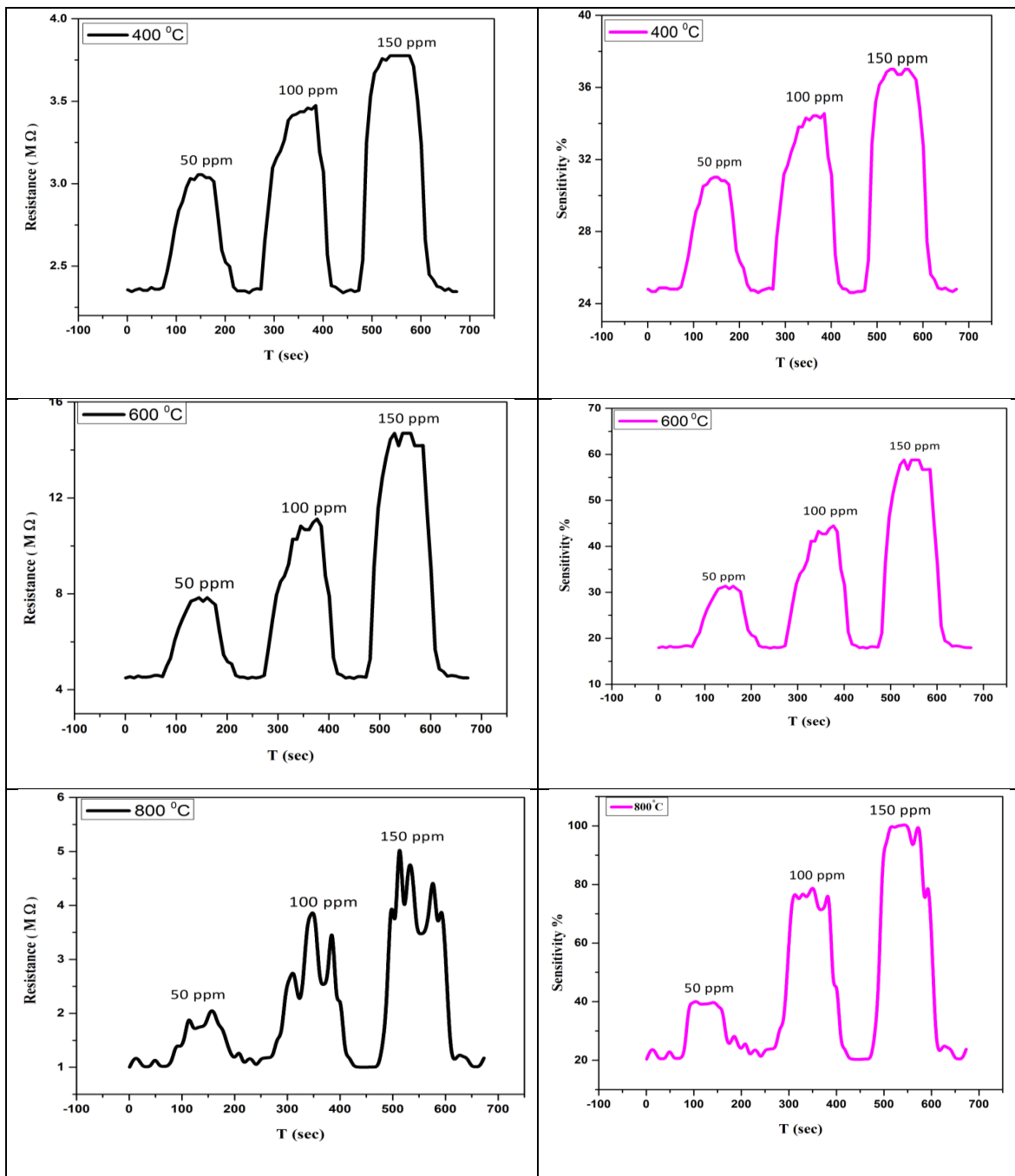


Fig. (8): Resistance and Sensitivity for the NO₂ gas for the samples that treated at different temperatures substrate 400°C, 600 °C and 800 °C,

Table (4): Gas sensor measurements

Temperature ⁰ C	Gas	Gas Concentration(ppm)	Sensitivity%
400	CO	50-100-150	40-55-70
	NH ₃	50-100-150	18-22-25
	NO ₂	50-100-150	31-34-37
600	CO	50-100-150	40-55-70
	NH ₃	50-100-150	30-44-60
	NO ₂	50-100-150	31-42-60
800	CO	50-100-150	65-70-81
	NH ₃	50-100-150	42-70-84
	NO ₂	50-100-150	40-80-100

From Table (4), we notice that with an increase in the gas concentration, the sensitivity increases, and the best sensitivity is at a temperature of 800 °C for all gases.

We note the high sensitivity of WO₃ thin films at the temperature of 800 °C due to the same time the increase in the surface roughness in this sample so that these two properties rise the surface area of the film and thus rise the area of the film subject to the reaction.

We also note that each sample has a certain temperature to reach the sensitivity, as the temperature of the membrane response decreases with the increase in surface roughness and the reason for that is n-type WO₃, it has a high number of electrons, so the adsorption of the gas on the surface of WO₃ it leads to trapping these electrons and thus obtaining a large change in resistance, which leads to an increase in the response due to an increase in the adsorption rate.

As for the other samples, we note that their response to the gas is less, and the reason for this is that the surface roughness is greatly reduced, and thus a decrease in the surface area of the reaction is achieved, and therefore the sensitivity of the films decreases by a large amount in some cases.

4-conclusion

With increased the temperatures substrate, the surface roughness of the samples increases, with increased the temperatures substrate, the crystallite size of the samples increases, with increased the temperatures substrate, the energy band gap of the samples decreases, with increased the temperatures substrate, absorbance spectra of the samples increases, with increased the temperatures substrate, transmittance spectra of the samples decreases and the best sensing to (NO₂) gas was recorded at the temperature substrate (800 °C) for high sensitivity (100%) at room temperature.

References

- [1] H.J. Chen, N.S. Xu, S.Z. Deng, D.Y. Lu, Z.L. Li, J. Zhou, J. Chen, "Synthesis of monoclinic WO₃ nanosphere hydrogen gasochromic film via a sol-gel approach using PS-b-PAA diblock copolymer as template", *Nanotechnology* 18 205701 China (2007).
- [2] Y. Hattori, S. Nomura, S. Mukasa, H. Toyota, T. Inoue, T. Kasahara, *J. Alloys Comp.*, "Synthesis of tungsten trioxide nanoparticles by microwave plasma in liquid", 560 (2013) 105–110 China (2017).
- [3] Y.X. Qin, F. Wang, W.J. Shen, M. Hu, *J. Alloys Comp.*, "Surface Modification of Titanium and Titanium Alloys: Technologies, Developments, and Future Interests", 540 21–26 Article in *Advanced Engineering Materials* (2020).
- [4] L. Fang, S.J. Baik, K.S. Lim, S.H. Yoo, M.S. Seo, S.J. Kang, J.W. Seo, *Appl. Phys. Lett.* 96 193501 Department of Physics, COMSATS University Islamabad (2010).
- [5] P. J. Barczuk, A. Krolikowska, A. Lewera, K. Miecznikowski, R. Solarska, J., "Structural and photoelectrochemical investigation of boron-modified nanostructured tungsten trioxide films", University of Warsaw (2013).
- [6] R. Sivakumar, A. Moses Ezhil Raj, B. Subramanian, M. Jayachandran Trivedi, C. Sanjeeviraja, *Mater. Res. Bull.*, "Preparation and characterization of spray deposited n-type WO₃ thin films for electrochromic devices", 39 1479–1489 Department of Physics, Scott Christian College, Nagercoil (2004).
- [7] Z. Silvester Houweling, John W. Geus, Michiel de Jong, Peter-Paul R.M.L. Harks, Karine H.M. van der Werf, Ruud E.I. Schropp, *Mater. Chem. Phys.* 131 (2011) 375–386.
- [8] K.J. Lethy, D. Beena, R.V. Kumar, V.P.M. Pillai, V. Ganesan, V. Sathe, *Appl. Surf. Sci.*, "Structural, optical and morphological studies on laser ablated nanostructured WO₃ thin films", *Sci.* 254 2369–2376 University of Kerala, Kariavattom (2008).

- [9] S. Yamamoto, A. Inouye, M. Yoshikawa, Nucl. Instrum. Methods B, "Gasochromic WO₃ Nanostructures for the Detection of Hydrogen Gas: An Overview", 266 802–806 University of Technology (2008).
- [10] L.M. Bertus, C. Faure, A. Danine, C. Labrugere, G. Campet, A. Rougier, A. Duta, "ynthesis and characterization of WO₃ thin films by surfactant assisted spray pyrolysis for electrochromic applications", Mater. Chem. Phys. 140 (2013) 49–59.
- [11] P.M. Kadam, N.L. Tanwal, P.S. Shinde, S. S. Mali, R.S. Patil, A.K. Bhosale, H.P. Deshmukh, P.S. Patil, "Enhanced optical modulation due to SPR in gold nanoparticles embedded WO₃ thin films", Journal of Alloys and Compounds, 509 (2011) 1729–1733.
- [12] W.L. Kwong, N. Savvides, C. C. Sorrell, "Electrodeposited nanostructured WO₃ thin films for photoelectrochemical applications", Electrochim. Acta 75 Australia (2012) 371–380
- [13] B. Ingham, S.V. Chong, J.L. Tallon, "Novel materials based on organic–tungsten oxide hybrid systems II: electronic properties of the W–O framework", Curr. Appl. Phys. 4 (2004) 202–205.
- [14] N. Naseri, H. Kim, W. Choi, A.Z. Moshfegh, "Implementation of Ag nanoparticle incorporated WO₃ thin film photoanode for hydrogen production", Int. J. Hydrogen Energy 38 (2013) 2117–2125.
- [15] R. Solarska, B.D. Alexander, A. Braun, R. Jurczakowski, G. Fortunato, M. Stiefel, T. Graule, J. Augustynski, "Tailoring the morphology of WO₃ films with substitutional cation doping: Effect on the photoelectrochemical properties", Electrochim. Acta 55 (2010) 7780–7787.
- [16] C.V. Ramana, G. Baghmar, E.J. Rubio, M.J. Hernandez, "Optical Constants of Amorphous, Transparent Titanium-Doped Tungsten Oxide Thin Films", ACS Appl. Mater. Int. 5 (2013) 4659–4666.
- [17] H.H. Lu, J. Alloys, "Effects of oxygen contents on the electrochromic properties of tungsten oxide films prepared by reactive magnetron sputtering", journal of alloys and Compounds, 465 (2008) 429–435.

- [18] S. Keshri, A. Kumar, D. Kabiraj, “Tailoring of optical and gas sensitivity behaviors of WO₃ films by low energy Ar⁺ ion implantation” , Thin Solid Films 526 (2012) 50–58.
- [19] K.J. Patel, C.J. Panchal, V.A. Kheraj, M.S. Desai, “Growth, structural, electrical and optical properties of the thermally evaporated tungsten trioxide (WO₃) thin films” , Mater. Chem. Phys. 114 475–478 (2009).
- [20] R. Binions, C. Piccirillo, R.G. Palgrave, I.P. Parkin, Chem. Vapor Depos. 14 (2008) 33–39. Kowalsky, J. Mater. Chem. 19 (2009) 702–705. , D.C.
- [21] A. I. Khudadad, “ Influence of thermal annealing on the gas sensing properties of Tungsten Oxide (WO₃) nano-sensor” , Mustansiriyah University,(2020).
- [22] J.W. Roberts, P.R. Chalker, B. Ding, R.A. Oliver, J.T. Gibbon, L.A.H. Jones, V.R. Dhanak, L.J. Phillips, J.D. Major, F.C.-P. Massabuau, “Low temperature growth and optical properties of α-Ga₂O₃ deposited on sapphire by plasma enhanced atomic layer deposition, Journal of Crystal Growth”, Volume 528, 2019, 125254(2019).